MODE-III SIFs IN STATIONARY AND DYNAMIC CRACKS TRAVERSING ORTHOTROPIC AND ISOTROPIC PLATES EVALUATED BY CAUSTICS

P. S. Theocaris and H. G. Georgiadis

Department of Theoretical and Applied Mechanics, The National Technical University of Athens, 5 Heroes of Polytechnion Avenue, Zographou, GR-157 73 Athens, Greece

ABSTRACT

The experimental method of reflected caustics, which was primarily developed to evaluate stress intensity factors for in-plane modes of deformation,was recently extended to calculate mode-III stress intensity factors in stationary cracks traversing isotropic plates submitted to antiplane shear. In this paper the method was extended to deal both with stationary cracks in orthotropic plates and propagating cracks in isotropic plates under mode-III.

KEYWORDS

Anti-plane deformation; elastic fracture mechanics; stress intensity factors; orthotropy; dynamic crack propagation; caustics.

NOTATION

(x_0,y_0), (r_0,ϑ_0)	cartesian and polar scaling coordinates in the orthotropic plate
(x_s,y_s), (r_s,ϑ_s)	cartesian and polar scaling coordinates fixed on the moving crack tip in the isotropic plate.
(x_i,y_i), (r_i,ϑ_i)	cartesian and polar scaling coordinates varying for each problem considered.
X,Y	cartesian coordinates on the screen
υ, c_s	crack and shear-wave velocities.
w	displacement normal to the xy-plane.
z_0	distance between the specimen and the screen.
z_i	distance between the focus of the light beam and the specimen.
$\alpha_s=[1-(\upsilon/c_s)^2]^{\frac{1}{2}}$	dynamic correction coefficient.
c_{44}, c_{55}	independent constants in the stiffness matrix.
$\lambda_m=(z_0+z_i)/z_i$	magnification factor of the optical arrangement.
Y_{max}	maximum transverse distance of the caustic curve from the crack axis.
$\alpha_0=(c_{55}/c_{44})^{\frac{1}{2}}$	ratio of shear stiffness in orthotropic bodies.

τ_{xz}, τ_{yz}	shear anti-plane stresses.
γ_{xz}, γ_{yz}	shear anti-plane strains.
G	shear modulus
K_{III}, $K_{III}(t)$	static and dynamic stress intensity factors in mode-III deformation.

INTRODUCTION

The optical method of reflected caustics was first applied to problems of cracked bodies (Theocaris, 1970,1971) or other stress singularities (Theocaris, 1973a,1973b) in stress fields subjected to an inplane mode of deformation. In this case, the deformation in the normal to the plate direction, developed because of the lateral contraction effect and/or the variation of the refractive index along the same direction, deviated the incident light in the vicinity of the crack tip and formed the caustic envelope. Later on, the method was extended to the study of the distribution of curvatures on plates and shells (Theocaris and Gdoutos, 1976) and stress fields in non-cracked and cracked plates under bending (Theocaris, 1977, 1982).

For the case of anti-plane shear deformation of a cracked thick plate none of the well-known optical experimental methods (photoelasticity, moiré, or transmitted caustics) could give information for the evaluation of the intensity of the stress- and displacement-field around the crack tip, since it is valid that $\sigma_x=\sigma_y=\sigma_z=\tau_{xy}=0$ and only the out-of-plane shear stresses τ_{xz} and τ_{yz} are operative, which do not create lateral normal deformation. However, it was shown that the method of reflected caustics was capable to detect and evaluate the K_{III}-stress intensity factor and it was established that the caustic formed by this type of deformation, is again a generalized epicycloid curve (Theocaris, 1981).

Among the other applications of the reflected caustics, which were appearing in the last decade, the case of a stationary crack traversing an anisotropic plate under in-plane loading was treated (Theocaris, 1976), which presents a great affinity with the caustics formed by propagating cracks in isotropic media, (Theocaris and Papadopoulos, 1980). On the other hand, an appreciable number of studies on dynamic fracture was investigated by this method. It was found that in both cases of orthotropic static cracks and isotropic dynamic cracks the shape and the size of the caustic curve formed on a screen for in-plane deformation, differs considerably from the common case of the isotropic static crack.

It remains to deal with the form and the size of caustics for stationary cracks in orthotropic plates and propagating cracks in isotropic plates under anti-plane shear and to evaluate the respective K_{III}-factors, and this is the subject of this paper. It is also shown that a complete similarity exists between the equations governing the latter problems if an appropriate scaling coordinate system will be used.

DISPLACEMENT-FIELD NEAR THE TIP OF A MODE-III STATIONARY CRACK TRAVERSING AN ORTHOTROPIC PLATE

Consider a thick orthotropic elastic plate, see Fig. 1, submitted to a convenient loading for anti-plane deformation (see for instance the configurations in pages 2.27, 4.10 and 5.1 of Tada, Paris and Irwin, 1973) and containing a stationary crack aligned with one, say the Ox, of the directions of orthotropy.

The only non-vanishing stresses are

$$\tau_{xz} = c_{55}\gamma_{xz}\ , \quad \tau_{yz} = c_{44}\gamma_{yz} \tag{1.1}$$

and the out-of-plane displacement w satisfies the equation

$$c_{55}\frac{\partial^2 w}{\partial x^2} + c_{44}\frac{\partial^2 w}{\partial y^2} = 0 \tag{1.2}$$

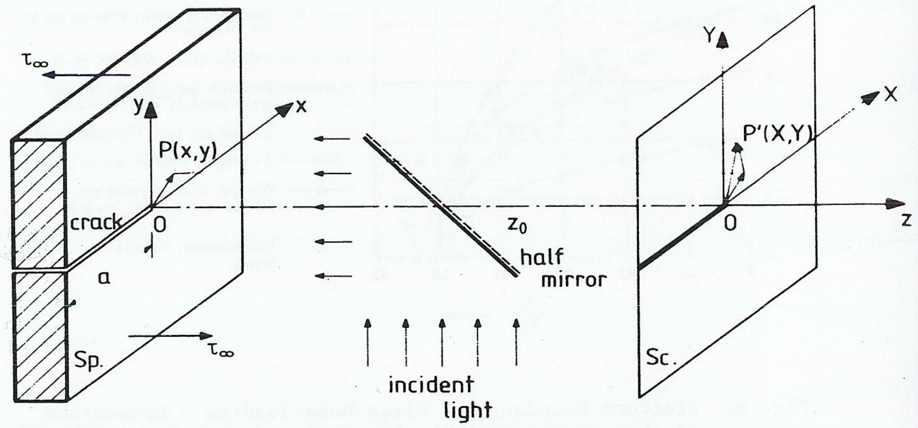

Fig. 1 A plate with an anti-plane shear crack and the viewing screen.

The near-tip displacement-field was given by Sih, Paris and Irwin (1965) in terms of polar coordinates r and ϑ in the physical plane

$$w = K_{III}\left(\frac{2r}{\pi}\right)^{\frac{1}{2}} \mathrm{Re}\left[\frac{(\cos\vartheta + \mu\sin\vartheta)^{\frac{1}{2}}}{\mu c_{44}}\right] \tag{2}$$

where

$$\mu = \pm\, i\left(\frac{c_{55}}{c_{44}}\right)^{\frac{1}{2}} \tag{3}$$

The displacement w, after some algebra, is expressed by

$$w(r,\vartheta) = \frac{K_{III}}{(\pi c_{44}c_{55})^{\frac{1}{2}}} r^{\frac{1}{2}}\left[\left(\cos^2\vartheta + \frac{c_{55}}{c_{44}}\sin^2\vartheta\right)^{\frac{1}{2}} - \cos\vartheta\right]^{\frac{1}{2}} \tag{4}$$

The above equation may be reduced to its *isotropic* counterpart when $c_{44}=c_{55}=G$, where G is the shear modulus of the material in any direction.
It is convenient to express the preceding relation in terms of the scaling coordinates

$$x_0 = x = r_0\cos\vartheta_0\ , \quad y_0 = \alpha_0 y = r_0\sin\vartheta_0\ , \quad z_0 = x + i\alpha_0 y \tag{5}$$

We may observe that

$$r = \left(r_0^2\cos^2\vartheta_0 + \frac{r_0^2\sin^2\vartheta_0}{\alpha_0^2}\right)^{\frac{1}{2}}$$

$$\cos^2\vartheta + \alpha_0^2\sin^2\vartheta = \frac{\alpha_0^2 r_0^2}{\alpha_0^2 r_0^2\cos^2\vartheta_0 + r_0^2\sin^2\vartheta_0} \tag{6}$$

Then, Eq.(4) takes the following simple form

$$w(r_0,\vartheta_0) = K_{III}\left(\frac{2r_0}{\pi c_{44}c_{55}}\right)^{\frac{1}{2}}\sin(\vartheta_0/2) \tag{7}$$

DISPLACEMENT-FIELD NEAR THE TIP OF A MODE-III PROPAGATING CRACK TRAVERSING AN ISOTROPIC PLATE

Attention is now focussed to a thick isotropic elastic plate, submitted to an anti-plane deformation and containing a propagating crack with constant velocity. It is assumed that the propagating crack expands at the Ox-axis in Fig. 1. The moving coordinates x,y, associated with the crack tip, are related to the static coordinates x'y' with the Galileian transformation $x=x'-\upsilon t$, $y=y'$. The near-tip displacement-field were given by Sih (1970) in terms of moving-polar coordinates r and ϑ in the physical plane. The same expression was also given by Nishioka and Atluri (1983) in terms of scaling moving-polar coordinates r_s and ϑ_s, as

$$w = \frac{K_{III}(t)}{G}\left(\frac{2r_s}{\pi}\right)^{\frac{1}{2}}\frac{1}{\alpha_s}\sin(\vartheta_s/2) \tag{8}$$

where

$$\tan\vartheta_s = \alpha_s\tan\vartheta \quad \text{and} \quad r_s = r[\cos^2\vartheta + \alpha_s\sin^2\vartheta]^{\frac{1}{2}} \tag{9}$$

In the above relation the dynamic or time-dependent $K_{III}(t)$-factor is an unknown scalar quantity, only determined by experimental methods.

THE REFLECTED CAUSTICS IN STATIONARY AND DYNAMIC CRACKS EXISTING IN ORTHOTROPIC AND ISOTROPIC PLATES

From the preceding analysis and especially from relations (7) and (8) we arrive to the conclusion that the governing equations of the two problems considered have the same functional form. Therefore, the searching for the size and shape of the reflected caustics formed by the displacement field for both of the two configurations can be jointly treated.

Using the symbol "i" as a suffix for similar parameters of the two problems, we take for i=s (dynamic case)

$$\alpha_i = \alpha_s = [1-\upsilon/c_s)^2]^{\frac{1}{2}}, \quad K^i_{III} = K_{III}(t), \quad F(\alpha_i) = 1/\alpha_s, \quad G_i = G \tag{10}$$

whereas, for i=0 (static case), we have

$$\alpha_i = \alpha_0 = (c_{55}/c_{44})^{\frac{1}{2}}, \quad K^i_{III} = K_{III}, \quad F(\alpha_i) = 1, \quad G_i = (c_{44}c_{55})^{\frac{1}{2}} \tag{11}$$

The reflected-caustic curve is obtained on a screen at a distance z_0 from the specimen, if a parallel (also convergent or divergent) light beam impinges on the lateral faces of the two lips of the anti-plane crack. The cylindrical curvature formed by the w-displacement deviates the reflected light according to Snellius' law and two distinct areas, one completely dark surrounded by a bright curve, and another illuminated, are created on the screen from the projections of either lip of the crack.

If w(x,y) expresses the function describing the deformed surface with respect to the undeformed lateral face of the plate, i.e. Eqs.(7) and (8) in our case, the caustic curve may be approximated by the following simplified equations (Theocaris, 1981)

$$X(x,y) = \lambda_m x - 2z_0\frac{\partial w(x,y)}{\partial x}, \quad Y(x,y) = \lambda_m y - 2z_0\frac{\partial w(x,y)}{\partial y} \tag{12}$$

The latter expressions may be written in terms of the scaling coordinates x_i, y_i as follows

$$X(x_i,y_i) = \lambda_m x_i - 2z_0\frac{\partial w(x_i,y_i)}{\partial x_i}, \quad Y(x_i,y_i) = \frac{\lambda_m y_i}{\alpha_i} - 2\alpha_i z_0\frac{\partial w(x_i,y_i)}{\partial y_i} \tag{13}$$

Finally, the equations of mapping in polar form are

$$X(r_i,\vartheta_i) = \lambda_m r_i\cos\vartheta_i + 2z_0\frac{K^i_{III}}{G_i(2\pi r_i)^{\frac{1}{2}}}\sin(\vartheta_i/2)F(\alpha_i) \tag{14.1}$$

$$Y(r_i,\vartheta_i) = \frac{\lambda_m r_i\sin\vartheta_i}{\alpha_i} - 2\alpha_i z_0\frac{K^i_{III}}{G_i(2\pi r_i)^{\frac{1}{2}}}\cos(\vartheta_i/2)F(\alpha_i) \tag{14.2}$$

High luminosity of the caustic curve, formed on the screen, implies that this curve is a singular mathematical curve. Therefore, the Jacobian determinant must be vanished, then it is valid

$$J = \frac{\partial(X,Y)}{\partial(x,y)} = 0 \tag{15}$$

The zeroing of the Jacobian determinant gives a function $r=r(\vartheta)$, called the *initial curve*, which has the property that every point inside or outside this curve maps outside the caustic in the (X,Y)-plane and every point on the initial curve maps on the caustic curve.

Then, from Eq.(15) we have

$$J = \frac{\partial(X,Y)}{\partial(x,y)} = \alpha_i\frac{\partial(X,Y)}{\partial(x_i,y_i)} = \alpha_i\frac{\partial(X(r_i,\vartheta_i),Y(r_i,\vartheta_i))}{\partial(r_i,\vartheta_i)} = 0 \tag{16}$$

We obtain for the Jacobian determinant

$$\frac{\partial(X,Y)}{\partial(r_i,\vartheta_i)} = \begin{vmatrix} \partial X/\partial r_i & \partial X/\partial\vartheta_i \\ \partial Y/\partial r_i & \partial Y/\partial\vartheta_i \end{vmatrix} = \lambda_m^2\frac{r_i}{\alpha_i} - \lambda_m c_i r_i^{-\frac{1}{2}}\sin(3\vartheta_i/2)\left(\frac{1-\alpha_i}{\alpha_i}\right) - \alpha_i c_i^2 r_i^{-2} \tag{17}$$

where

$$c_i = \frac{z_0 K^i_{III}F(\alpha_i)}{G_i(2\pi)^{\frac{1}{2}}} \tag{18}$$

Inserting Eq.(17) into (16) we derive the equation for the initial curve

$$r_{i,0} = \left\{ \frac{c_i \sin(3\vartheta_i/2)(1-\alpha_i)+c_i[\sin^2(3\vartheta_i/2)(1-\alpha_i)^2+4\alpha_i^2]^{1/2}}{2\lambda_m} \right\}^{2/3} \tag{19}$$

One may observe that Eqs.(14),(17) and (19) are reduced to the respective equations prevailing for a stationary crack in an isotropic plate under mode-III deformation when $\alpha_i=1$ and $c_{44}=c_{55}=G$.

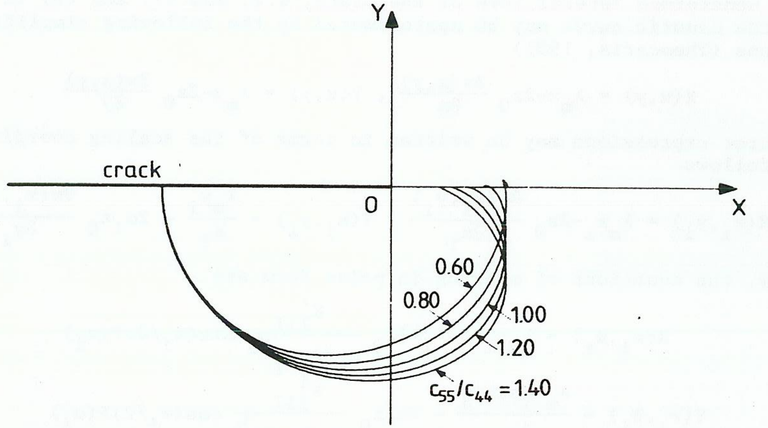

Fig. 2. Caustic curves for a static crack traversing an orthotropic plate.

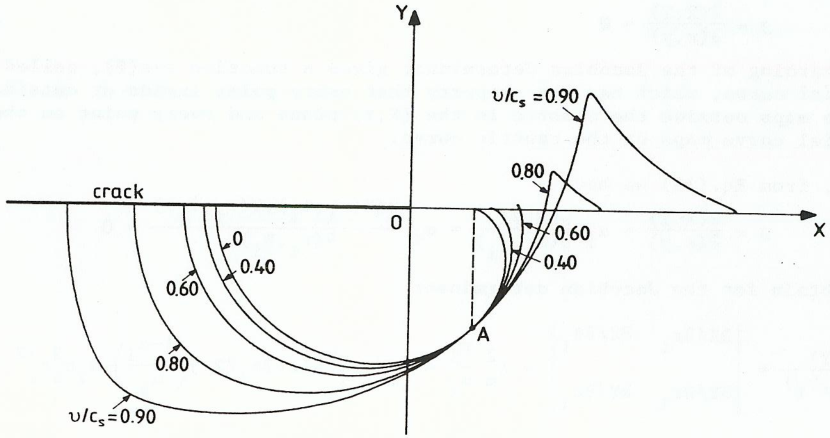

Fig. 3. Caustic curves for a dynamic crack traversing an isotropic plate.

Fig. 2 presents caustic curves for the case of a *static orthotropic* crack as

they have been plotted by the computer. The ratio $c_{55}/c_{44}=G_{xz}/G_{yz}$ ranges between 0.60 and 1.40. Fig. 3 presents caustic curves theoretically obtained for the case of a *dynamic* and *isotropic* crack and for constant velocity. The ratio υ/c_s ranges between 0 and 0.90. In both cases the K_{III}^i-factor is kept constant in order to examine the effect of orthotropy and velocity in the shape and the size of the caustics.

EVALUATION OF THE TRANSVERSE DISTANCES Y_{max} OF THE CAUSTICS AND THE RESPECTIVE K_{III}^i-FACTOR

Relation (14.2) presents extrema, which may be found by zeroing the derivative $\partial Y(\vartheta_i)/\partial\vartheta_i$.

Thus we have

$$\frac{\partial Y(\vartheta_i)}{\partial\vartheta_i} = \lambda_m^{1/3} c_i^{2/3} \Big(\frac{0.63}{\alpha_i} \cos\vartheta_i R^{2/3} + \frac{0.42}{\alpha_i} \sin\vartheta_i R^{-1/3} R^* + 1.26\alpha_i \sin(\vartheta_i/2) \cdot$$
$$\cdot R^{-1/3} + 0.84\alpha_i \cos(\vartheta_i/2) R^{-4/3} R^* \Big) = 0 \tag{20}$$

with

$$R = \sin(3\vartheta_i/2)(1-\alpha_i)+[\sin^2(3\vartheta_i/2)(1-\alpha_i)^2+4\alpha_i^2]^{1/2} \tag{21.1}$$

$$R^* = \frac{\partial R}{\partial\vartheta} = \frac{3}{2}(1-\alpha_i)\cos(3\vartheta_i/2)\{1+(1-\alpha_i)[\sin^2(3\vartheta_i/2)(1-\alpha_i)^2+4\alpha_i^2]^{-1/2}\sin(3\vartheta_i/2)\} \tag{21.2}$$

Eq.(20) has been solved with the computer and gives the value of $\vartheta_i=\vartheta_i^{max}$ for which the transverse distance takes its maximum Y_{max}. This quantity may be written in the form

$$Y_{max} = \lambda_m^{1/3} c_i^{2/3} \delta_i^{max} \tag{22}$$

where

$$\delta_i^{max} = \left\{ \frac{\sin\vartheta_i^{max}}{\alpha_i} \left(\frac{R^{max}}{2}\right)^{2/3} - 2\alpha_i \cos(\vartheta_i^{max}/2) \left(\frac{R^{max}}{2}\right)^{-1/3} \right\} \tag{23}$$

is a correction factor given in the diagram of Fig. 4 for various ratios of (c_{55}/c_{44}) and (υ/c_s).

From Eq.(18) and (22) the relation, which connects the K_{III}^i-factor with the material constants and the experimental data and the appropriate parameters, is given by

$$K_{III}^i = \frac{G_i(2\pi)^{1/2}}{\lambda^{1/2} z_0 F(\alpha_i)} \left(\frac{Y_{max}}{\delta_i^{max}}\right)^{3/2} \tag{24}$$

Thus, with one simple measurement of the maximum transverse distance of the experimental caustic from the crack-axis and by using the diagram of Fig. 4 and relation (24) one may evaluate the stress intensity factors of the anti-plane problems considered in this paper.

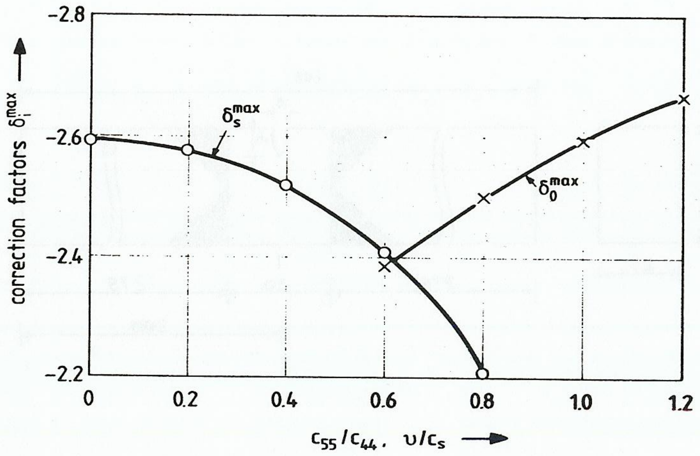

Fig. 4. Correction factors δ_0^{max} and δ_s^{max} versus (c_{55}/c_{44}) and (υ/c_s) respectively.

REFERENCES

Nishioka, T., and S.N. Atluri (1983). *Engng. Fract. Mech.*, 18(1), 1-22.

Sih, G.C. (1970). In *Inelastic Behaviour of Solids*, (ed. M.F. Kanninen and others), McGraw-Hill.

Sih, G.C., P.C. Paris, and G.R. Irwin (1965). *Int. J. Fracture*, 1, 189-203.

Tada, H., P.C. Paris, and G.R. Irwin (1973). *The Stress Analysis of Cracks Handbook*, Del Research Corporation, Penn.

Theocaris, P.S. (1970). *J. Appl. Mech.*, 37, *Trans. ASME*, 92E, 409-415.

Theocaris, P.S. (1971). *Appl. Optics*, 10, 2240-2247.

Theocaris, P.S. (1973a). *Appl. Optics*, 12, 380-387.

Theocaris, P.S. (1973b). *Exp. Mechanics*, 13, 511-518.

Theocaris, P.S. (1976). *J. Strain Analysis*, 11(3), 154-160.

Theocaris, P.S. (1977). *Int. J. Solids Structures*, 13(4), 1281-1291.

Theocaris, P.S. (1981). *Int. J. Mech. Sci.*, 23, 105-117.

Theocaris, P.S. (1982). *J. Appl. Mech.*, 49, 87-96.

Theocaris, P.S., and E.E. Gdoutos (1976). *Appl. Optics*, 15(6), 1629-1638.

Theocaris, P.S., and G.A. Papadopoulos (1980). *Engng. Fract. Mech.*, 13, 683-698.